Available online at www.sciencedirect.com
SCIENCE DIRECT®
ELSEVIER
Biochemical and Biophysical Research Communications 336 (2005) 223–231
BBRC
www.elsevier.com/locate/ybbrc

Spatial microenvironment defines Ca^{2+} entry and Ca^{2+} release in salivary gland cells

Haruo Takemura *, Yoshiyuki Horio

Department of Pharmacology, Sapporo Medical University, South 1, West 17, Sapporo 060-8556, Japan

Received 22 July 2005
Available online 19 August 2005

Abstract

The difference of Ca^{2+} mobilization induced by muscarinic receptor activation between parotid acinar and duct cells was examined. Oxotremorine, a muscarinic–cholinergic agonist, induced intracellular Ca^{2+} release and extracellular Ca^{2+} entry through store-operated Ca^{2+} entry (SOC) and non-SOC channels in acinar cells, but it activated only Ca^{2+} entry from non-SOC channels in duct cells. RT-PCR experiments showed that both types of cells expressed the same muscarinic receptor, M3. Given that ATP activated the intracellular Ca^{2+} stores, the machinery for intracellular Ca^{2+} release was intact in the duct cells. By immunocytochemical experiments, IP_3R2 colocalized with M3 receptors in the plasma membrane area of acinar cells; in duct cells, IP_3R2 resided in the region on the opposite side of the M3 receptors. On the other hand, purinergic P2Y2 receptors were found in the apical area of duct cells where they colocalized with IP_3R2. These results suggest that the expression of the IP_3Rs near G-protein-coupled receptors is necessary for the activation of intracellular Ca^{2+} stores. Therefore, the microenvironment probably affects intracellular Ca^{2+} release and Ca^{2+} entry.

Keywords: Acinar and duct cells; Ca^{2+} entry; Ca^{2+} release; IP_3 receptor; M3 receptor; P2Y receptor; Microenvironment

Increases in the cytoplasmic Ca^{2+} concentration ($[Ca^{2+}]_i$) regulate many cellular functions such as proliferation, transcription, metabolism, contraction, and exocytosis [1]. The stimulation of G-protein Gq-coupled receptors activates phospholipase Cβ (PLCβ), resulting in the hydrolysis of phosphatidylinositol 4,5-bisphosphate and the production of inositol 1,4,5-trisphosphate (IP_3) and diacylglycerol (DAG). IP_3 binds its receptors on the intracellular Ca^{2+} store and releases Ca^{2+} from the store, causing the first phase of an increase in $[Ca^{2+}]_i$. The second phase is Ca^{2+} entry from the extracellular medium into the cell; this phase maintains a high level of $[Ca^{2+}]_i$. Extracellular Ca^{2+} entry after Gq-coupled receptor stimulation is mediated by two mechanisms. One is store-operated Ca^{2+} entry (SOC) and the other is non-store-operated Ca^{2+} entry (non-SOC). SOC channels, which are activated by the depletion of intracellular Ca^{2+} stores, are assumed to provide a major pathway for such Ca^{2+} entry [2]. Many cells also express non-SOC channels, which are activated by Gq-coupled receptor stimulation and support Ca^{2+} entry from the extracellular space. Non-SOC channels cannot be activated by store depletion, but some of them are opened by DAG [3,4]. Electrophysiological and pharmacological experiments have shown that there are multiple SOC and non-SOC channels that are expressed in various types of cells.

The salivary gland is an exocrine organ capable of secreting fluid and enzymes, and is regulated by autonomic nerves. It is made of tubular epithelia that are divided into two major domains. The distal end is the acinar unit, which produces the primary saliva, including the fluid and macromolecules. The proximal area is a duct that is thought to modify the primary saliva by absorbing and/or secreting electrolytes such as Na^+, Cl^-, and HCO_3^- [5,6]. The secretion and modification of saliva in the acini and ducts are triggered by the elevation of $[Ca^{2+}]_i$. Acetylcholine (ACh)

* Corresponding author. Fax: +81 11 612 5861.
E-mail address: takemura@sapmed.ac.jp (H. Takemura).

0006-291X/$ - see front matter © 2005 Elsevier Inc. All rights reserved.
doi:10.1016/j.bbrc.2005.07.200

is one of the most potent physiological stimulators of salivary glands. Muscarinic receptor stimulation induces the elevation of $[Ca^{2+}]_i$ in both acinar and duct cells. Using isolated rat parotid acini and ducts we found previously that carbachol, a muscarinic receptor agonist, induced Ca^{2+} release from intracellular stores and extracellular Ca^{2+} entry in acinar cells, but it activated only Ca^{2+} entry in duct cells [7].

In the present study, we examined and compared the difference in the $[Ca^{2+}]_i$ increase resulting from the stimulation of muscarinic receptors in parotid acinar and duct cells. Oxotremorine (OXO), a muscarinic–cholinergic agonist, induced intracellular Ca^{2+} release and extracellular Ca^{2+} entry through SOC and non-SOC channels in acinar cells, but it activated only Ca^{2+} entry from non-SOC channels in duct cells. In contrast, ATP released Ca^{2+} from the stores and activated both the SOC and non-SOC channels of duct cells. RT-PCR experiments showed that both types of cells expressed the same muscarinic receptor, M3. By immunocytochemical experiments, IP_3R2 colocalized with M3 receptors near the plasma membranes of acinar cells; in duct cells, IP_3R2 resided near the membrane opposite the M3 receptors. On the other hand, purinergic P2Y2 receptors were found in the apical area of duct cells where they colocalized with IP_3R2. These results indicate that G-protein-coupled receptors and the Ca^{2+} release machinery may need to be close to one another for Ca^{2+} to be released from the stores or enter from the extracellular space.

Materials and methods

Reagents. Fluo-3/AM and anti-goat Alexa 488 were obtained from Molecular Probes. Collagenase (type 4) was from Worthington. Anti-M3 receptor antibody, anti-mouse FITC, and anti-rabbit FITC were from Santa Cruz. Anti-IP3R2 mAb was a gift from Dr. K. Mikoshiba. Anti-P2Y2 antibody was from Alomone. Other chemicals were from Sigma.

Isolation of acini and ducts. The Animal Welfare Guidelines of Sapporo Medical University were followed in all the studies and experiments. Parotid acini and ducts were isolated from male Wistar rats (4–5 weeks old) as described previously [7,8]. Briefly, the parotid gland was removed, trimmed of the connective tissue, and cut into small pieces. They were digested with collagenase (2 mg/ml) in serum-free Dulbecco's modified Eagle's medium (DMEM) for 20 min at 37 °C with constant shaking and gentle pipetting. The isolated acini and ducts were incubated with Fluo-3/AM (10 μM) for 20 min in DMEM at 37 °C. After washing, the acini and ducts were resuspended in Krebs–Ringer–Hepes medium (KRH) containing 0.2% BSA. The composition of KRH was as follows: 120 mM NaCl, 5.4 mM KCl, 1.0 mM $CaCl_2$, 0.8 mM $MgCl_2$, 11.1 mM glucose, and 20 mM Hepes (pH 7.4). In the experiments performed in the absence of extracellular Ca^{2+}, Ca^{2+}-free KRH containing 0.2 mM EGTA was used.

RT-PCR. To purify total RNA from acinar and duct cells, several clusters of acini and several small duct fragments were collected in glass micropipettes under microscopic examination. Typical microscopic images of a cluster of acini and a duct fragment are shown in Figs. 1A and B, respectively. Collected acini and ducts were transferred to clean microcentrifuge tubes and broken up by three freeze-thaw cycles. Total RNA was purified from these acini and ducts using an RNeasy Mini Kit (Qiagen). cDNAs were synthesized for 60 min at 42 °C using 200 U of Superscript II RNase H^- Reverse Transcriptase (Invitrogen).

The primers to amplify α-amylase, kallikrein, GAPDH, and M1–M5 were used (see Supplemental information for sequences). PCR was carried out in a GeneAmp PCR System 9700 (Applied Biosystems). The thirty amplification cycles for α-amylase, kallikrein, and GAPDH were conducted with denaturation at 94 °C for 30 s, annealing at 55 °C for 1 min, and extension at 72 °C for 1 min, followed by a final extension at 72 °C for 5 min. The cycling conditions for M1–M5 were 35 cycles of 94 °C for 1 min, 55 °C for 1 min, and 72 °C for 1 min. A second set of nested primers, which immediately followed the first set of primers in their sequences, was used. For the reaction, 1 μl of the PCR product from the first round of amplification (20 μl) was used as a template for the second round of amplification. The PCR conditions were the same as in the first round. The resulting PCR mixtures were then analyzed by gel electro-

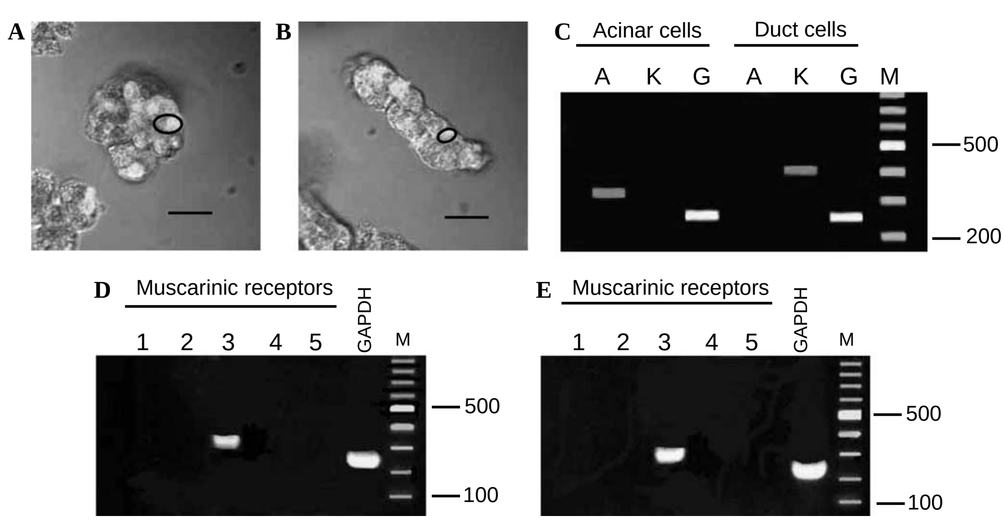

Fig. 1. Acini and ducts were isolated from the parotid gland by digestion with collagenase. (A,B) Typical images of an acinar cluster and a duct fragment loaded with Fluo-3, respectively. Circles show single cells whose Ca^{2+} responses are shown in Figs. 2A and B. Bar: 20 μm. (C) RT-PCR of α-amylase and kallikrein. α-Amylase is a marker enzyme for acinar cells and kallikrein is a marker for duct cells. Lane A, α-amylase. Lane K, kallikrein. Lane G, glyceraldehyde 3-phosphate dehydrogenase (GAPDH). (D,E) RT-PCR of muscarinic receptors. Muscarinic receptor subtype 3 was detected in both acinar (D) and duct (E) cells.

phoresis on 2% agarose gels. PCR products in the gel were stained by CYBR Green I Nucleic Acid Gel Stain (Cambrex).

Analysis of the intracellular Ca^{2+} signals by confocal laser scanning microscopy. Fluo-3-loaded acini and ducts were placed in a 35-mm glass-bottomed dish (Matsunami) as described previously [9]. The intracellular Ca^{2+} signals were measured using a time-lapse confocal laser scanning microscope (LSM510, Carl Zeiss) as reported previously [8,7]. An Ar/Kr laser was used to excite the Fluo-3 at 488 nm, and emission signals were collected through a 515-nm barrier filter. The acini and ducts were stimulated by perifusion with KRH containing OXO at 37 °C and viewed with a Zeiss 63 × /1.3 NA oil immersion objective.

Immunofluorescence microscopy of M3 receptors, IP_3 receptors, and P2Y2 receptors. Dissociated acini and ducts were fixed with 4% paraformaldehyde for 2 h. For cryosectioning, tissues were cryoprotected with 10–30% sucrose in PBS, embedded in Tissue Tek O.C.T. compound (Sakura Finetek, Torrance, California), and frozen in liquid nitrogen. Cryosections (12 μm) were permeabilized with 0.05% Triton X-100 in PBS and treated with PBS containing 1% BSA for 30 min at room temperature. These sections were then incubated with a goat polyclonal antibody against the M3 receptor (1:400), mouse monoclonal antibody against IP_3R2 (1:600), or polyclonal antibody against the P2Y2 receptor (1:200). After being washed, the sections were incubated with Alexa 488-conjugated anti-goat IgG, FITC-conjugated anti-mouse IgG, or FITC-conjugated anti-rabbit IgG and observed under a laser scanning confocal fluorescence microscope (Radiance 2100, Bio-Rad).

Results

M3 muscarinic receptors in acinar and duct cells

Carbachol does not induce Ca^{2+} release from intracellular stores in duct cells, although it does so in acinar cells [7]. To investigate this difference between acinar and duct cells, the subtypes of muscarinic receptors were examined in these cells using RT-PCR. The dissociated acinar and duct cells from rat parotid glands could easily be identified by their morphology. Representative images of acinar and duct preparations are shown in Figs. 1A and B, respectively. Total RNA was isolated from these preparations. To determine the amount of cross-contamination in these preparations, RT-PCR experiments were performed to detect α-amylase and kallikrein, which are, respectively, acinar and duct cell markers (Fig. 1C). α-Amylase was detected in the preparation from acini but not in that from ducts, whereas kallikrein was found only in ducts. Previously, acinar cells were reported to express the M3 muscarinic receptor [10,11], but the muscarinic receptor subtype in duct cells has been unknown. The muscarinic receptor

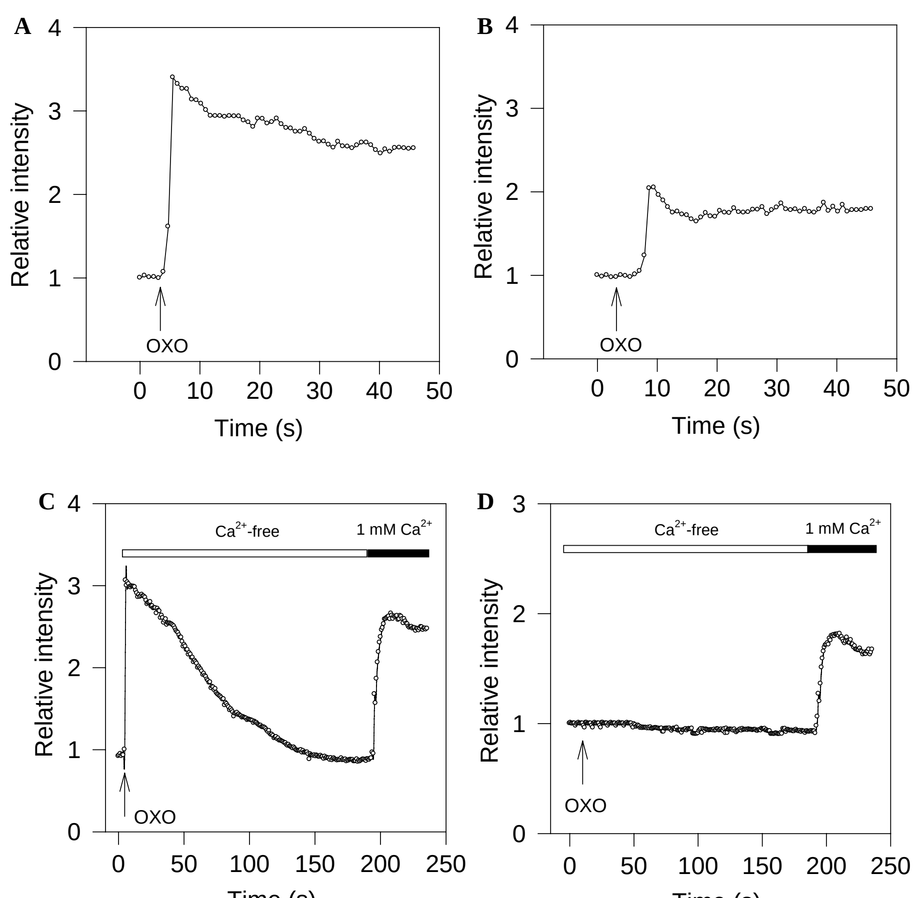

Fig. 2. Ca^{2+} responses of the acinar and duct cells circled in Figs. 1A and B are shown in (A) and (B), respectively. Each trace is a representative result from more than 10 records. The fluorescence changes of Fluo-3-loaded cells were detected using a confocal laser scanning microscopic system. Fluorescence intensity is indicated as the relative intensity (fold above the resting level of fluorescence before adding the drug). (A,B) Ca^{2+} responses of acinar (A) and duct (B) cells in the presence of 1 mM Ca^{2+}. Oxotremorine (OXO, 100 μM) was added at arrows. (C,D) Ca^{2+} responses of acinar (C) and duct (D) cells in Ca^{2+}-free KRH containing 0.2 mM EGTA. Subsequently, 1 mM Ca^{2+} was added (filled bar).

subtypes were examined in the acinar and duct cells. As shown in Figs. 1D (acini) and E (ducts), both the acini and ducts expressed only the M3 receptor among the five subtypes of muscarinic acetylcholine receptors tested.

Different Ca^{2+} responses of acini and ducts to muscarinic receptor stimulation

To examine the differences in the Ca^{2+} responses of the two cell types precisely, muscarinic agonist OXO (100 μM) was added to isolated acinar and duct cells (circled in Figs. 1A and B); their responses are shown in Figs. 2A (acinar cell) and B (duct cell). $[Ca^{2+}]_i$ rapidly increased and reached a peak within 1 s of the addition of OXO to the acinar cells. The $[Ca^{2+}]_i$ in the cells then slightly decreased and was maintained at a plateau level. OXO also increased $[Ca^{2+}]_i$ in the duct cells, but the onset of the increase was slower. The time lag to the start of $[Ca^{2+}]_i$ elevation between the acinar and duct cells was about 3 s. The level of increase in $[Ca^{2+}]_i$ in acinar cells was larger than in duct cells.

The difference in the increase of $[Ca^{2+}]_i$ between acinar and duct cells was further examined in the absence of extracellular Ca^{2+}. OXO induced a transient increase in $[Ca^{2+}]_i$ in acinar cells, which then declined to the resting level, indicating that Ca^{2+} was released from the intracellular stores (Fig. 2C). The subsequent addition of extracellular Ca^{2+} (1 mM) elevated the $[Ca^{2+}]_i$. In contrast, OXO did not induce any increase of $[Ca^{2+}]_i$ in the duct cells in the absence of extracellular Ca^{2+} (Fig. 2D). The subsequent addition of extracellular Ca^{2+} caused an increase in $[Ca^{2+}]_i$. Thus, intracellular Ca^{2+} release was absent, but extracellular Ca^{2+} entry could be induced by OXO in duct cells.

Effect of gadolinium ion (Gd^{3+}) on Ca^{2+} entry in acinar and duct cells

Gd^{3+} is a pharmacological tool that can be used to distinguish SOC and non-SOC channels [12,13]. A low concentration of Gd^{3+} (1 μM) selectively inhibits SOC channels, whereas a high concentration (100 μM) suppresses both SOC and non-SOC channels [12,13]. Whether 1 μM Gd^{3+} actually inhibits SOC channels of parotid glands was examined. SOC channels are activated by intracellular store depletion of Ca^{2+} with thapsigargin [14]. Acinar and duct cells were pretreated with 1 μM

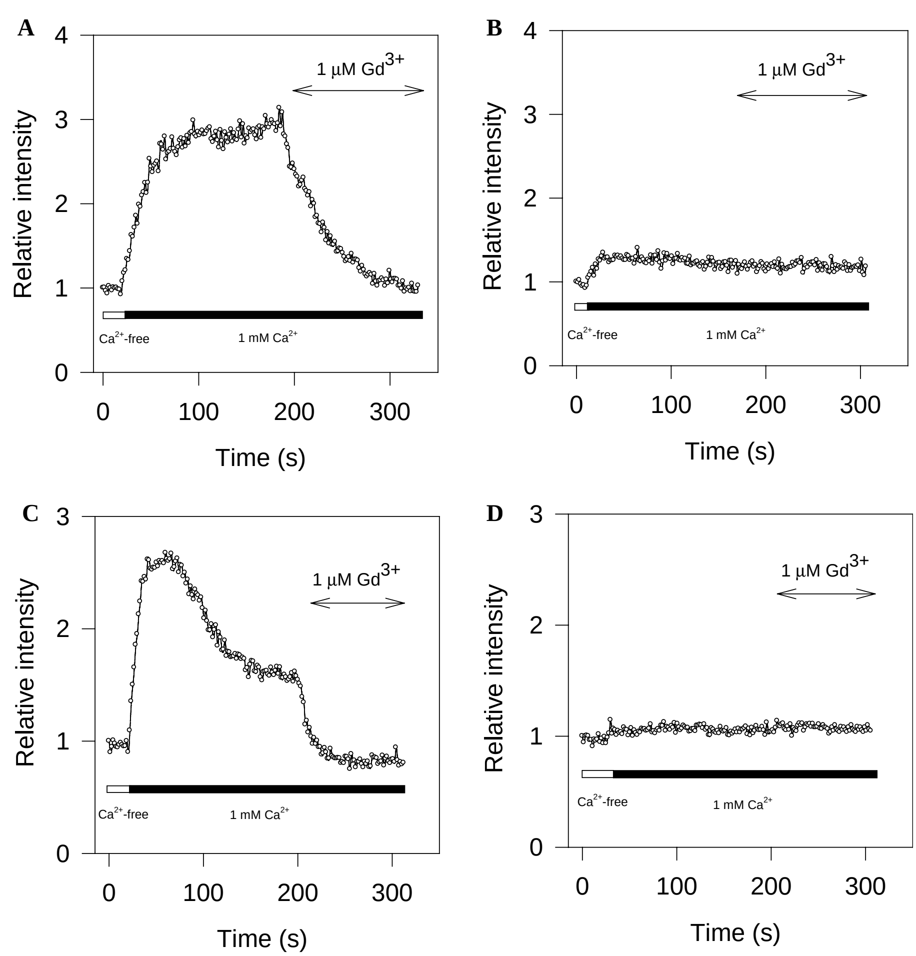

Fig. 3. Inhibition of store-operated Ca^{2+} entry by a low concentration of Gd^{3+} in acinar and duct cells. Acinar (A,B) and duct (C,D) cells were pretreated with 0.1% dimethyl sulfoxide (A,C) or 1 μM thapsigargin (B,D) in Ca^{2+}-free KRH containing 0.2 mM EGTA for 5 min, followed by the addition of 1 mM Ca^{2+}. A low concentration (1 μM) of Gd^{3+} was added at the plateau level. Each trace is a representative result from more than six records.

thapsigargin in Ca^{2+}-free KRH for 5 min, and then 1 mM Ca^{2+} was added to the extracellular medium (Fig. 3). The addition of Ca^{2+} increased $[Ca^{2+}]_i$ and $[Ca^{2+}]_i$ reached a plateau level in acinar cells (Fig. 3A). Surprisingly, duct cells also increased $[Ca^{2+}]_i$ after addition of extracellular Ca^{2+} (Fig. 3C). $[Ca^{2+}]_i$ reached a peak, after which it decreased and was maintained at a plateau level in duct cells. Thus, functional SOC channels also exist in duct cells. A low concentration of Gd^{3+} completely inhibited a plateau level of Ca^{2+} in both cell types. In the absence of thapsigargin, 1 μM Gd^{3+} had no effect on $[Ca^{2+}]_i$ in acinar and duct cells (Figs. 3B and D). These results show that functional SOC channels exist in acinar and duct cells.

Next, whether Gd^{3+} inhibits Ca^{2+} entry evoked by OXO in acinar and duct cells was checked. A low concentration of Gd^{3+} partially inhibited the plateau level of $[Ca^{2+}]_i$ evoked by OXO in acinar cells (Fig. 4A). The subsequent addition of the high concentration of Gd^{3+} completely suppressed the sustained increase in $[Ca^{2+}]_i$. On the other hand, the high, but not the low, concentration of Gd^{3+} inhibited extracellular Ca^{2+} entry induced by OXO into duct cells (Fig. 4B). These data indicate that the stimulation of M3 receptors activates both SOC and non-SOC channels in acinar cells, but it opens only non-SOC channels in duct cells.

DAG has been reported to activate some non-SOC channels [12,13]. Whether non-SOC channels in acinar and duct cells could be activated by DAG was further examined using 1-oleoyl-2-acetyl-*sn*-glycerol (OAG), a membrane-permeable DAG analogue. In the presence of extracellular Ca^{2+}, OAG (100 μM) increased $[Ca^{2+}]_i$ very slowly in acinar and duct cells (data not shown). When extracellular Ca^{2+} was omitted, OAG did not increase $[Ca^{2+}]_i$ in either type of cell. $[Ca^{2+}]_i$ was rapidly increased by the subsequent addition of extracellular Ca^{2+} and reached a plateau in both acinar (Fig. 4C) and duct (Fig. 4D) cells. One micromolar Gd^{3+} had no effect on $[Ca^{2+}]_i$, but a high concentration of Gd^{3+} blocked the Ca^{2+} entry (Figs. 4C and D). These results indicate that both types of cells expressed similar DAG-sensitive non-SOC channels.

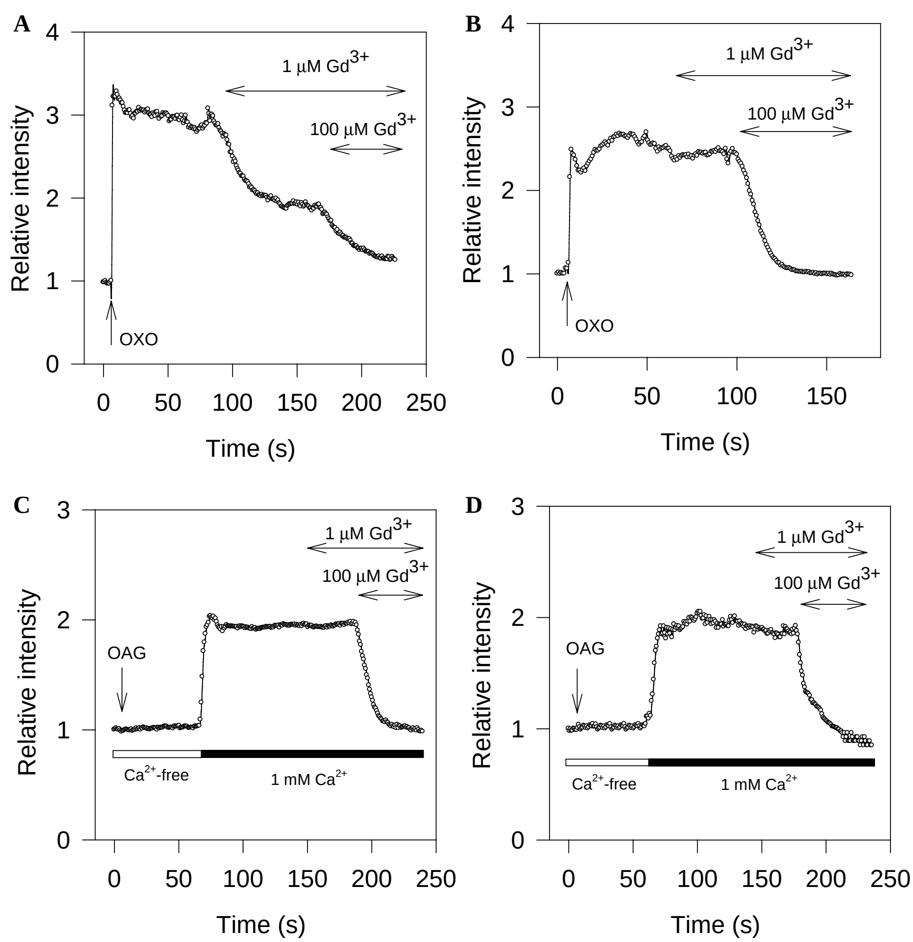

Fig. 4. Effects of Gd^{3+} on Ca^{2+} entry induced by OXO and DAG in acinar and duct cells. (A,B) OXO (100 μM) was added at the time of the arrows to acinar (A) and duct (B) cells, followed by low (1 μM) and high (100 μM) concentrations of Gd^{3+}. (C,D) 1-Oleoyl-2-acetyl-*sn*-glycerol (OAG, 100 μM) was added at the time of the arrows to acinar (C) and duct (D) cells in Ca^{2+}-free KRH containing 0.2 mM EGTA, followed by the addition of 1 mM Ca^{2+}. Low and high concentrations of Gd^{3+} were added at the plateau level. Each trace is a representative result from more than six records.

Activation of duct cell intracellular Ca^{2+} stores and SOC channels by ATP

We previously reported that ATP increased $[Ca^{2+}]_i$ in the duct cells of the rat parotid gland [7]. ATP was used to explore the existence of Ca^{2+} stores and SOC channels in duct cells. In the absence of extracellular Ca^{2+}, ATP (100 μM) induced a transient increase in $[Ca^{2+}]_i$, indicating that Ca^{2+} was released from intracellular stores (Fig. 5A). The subsequent addition of extracellular Ca^{2+} further increased $[Ca^{2+}]_i$. The increase in $[Ca^{2+}]_i$ may have been due to the activation of SOC channels. As shown in Fig. 5B, 1 μM Gd^{3+} partially inhibited the plateau level of $[Ca^{2+}]_i$ induced by ATP and the subsequent addition of 100 μM Gd^{3+} completely suppressed the increase in $[Ca^{2+}]_i$ in duct cells. Thus, our results indicated that ATP activates Ca^{2+} release from the intracellular stores and extracellular Ca^{2+} entry through SOC and non-SOC channels.

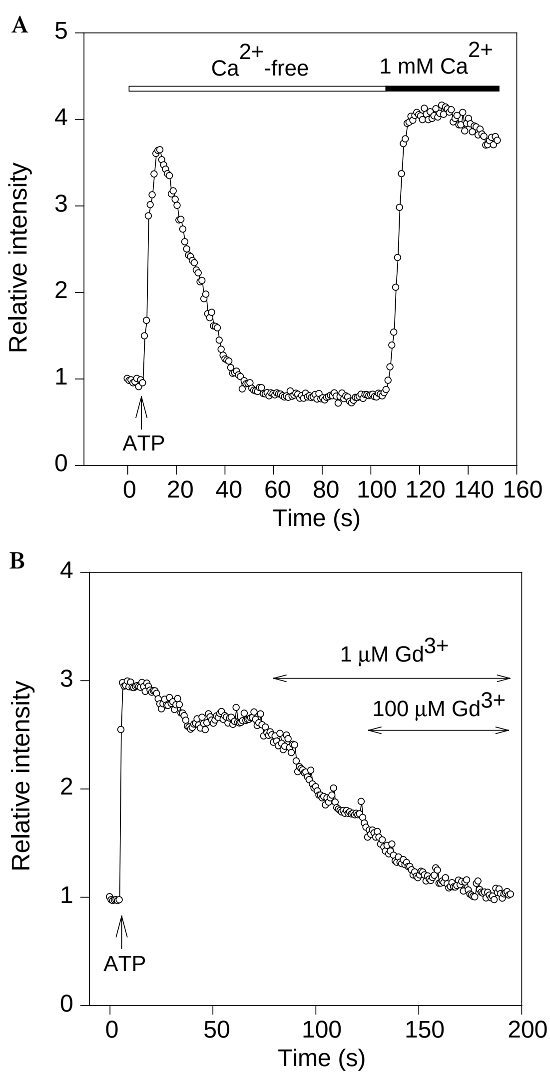

Fig. 5. Effects of ATP on Ca^{2+} release and Ca^{2+} entry in duct cells. (A) ATP (100 μM) was added at the time of the arrow to duct cells in Ca^{2+}-free KRH containing 0.2 mM EGTA, followed by the addition of 1 mM Ca^{2+}. (B) ATP (100 μM) was added at the time of the arrow to cells in the presence of extracellular Ca^{2+} and then low (1 μM) and high (100 μM) concentrations of Gd^{3+} were added. Each trace is a representative result from more than eight records.

Localization of IP_3R2, M3 receptors, and P2Y2 receptors in acinar and duct cells

Both acinar and duct cells expressed the same M3 receptor. In acinar cells, the intracellular Ca^{2+} release and SOC channels were activated by the M3 receptor stimulation, but those of the duct cells did not function in the same way in response to M3 receptor activation. This led to the question. What is the difference between acinar and duct cells? One possibility was if the distribution of M3 receptors and IP_3Rs differed in duct and acinar cells, M3 receptor signals in duct cells might not reach the intracellular Ca^{2+} stores. Previous experiments showed that IP_3R2 was the dominant IP_3R subtype in the acini and duct cells of the salivary gland [15]. By immunocytochemistry, the distribution of IP_3R2 in the duct cells was distinct from that in acinar cells (Fig. 6A). Acinar cells expressed IP_3R2 in the basal as well as the apicolateral areas, indicating that IP_3R2 is expressed globally in the region of the plasma membrane. On the other hand, IP_3R2 was found only in the apical (luminal) region of duct cells and was not seen in the area of the basal or lateral membranes (Fig. 6A).

The immunohistochemical distribution of M3 receptors was compared with that of IP_3R2 in the parotid salivary glands. As shown in Fig. 6B, the M3 receptors were expressed in the basal and apicolateral regions of acinar cells, suggesting that the M3 receptors in these cells were close to the IP_3R2. In contrast, the M3 receptors of duct cells were found in basal area but not in the apicolateral area. Thus, the M3 receptors in duct cells were located in the region of the opposite side of the membrane from IP_3R2.

ATP induced Ca^{2+} release from the intracellular stores and opened both the SOC and non-SOC channels in duct cells (Fig. 5). P2Y purinergic receptors activate Gq proteins and PLCβ in response to ATP. Among the P2Y receptors, the P2Y2 and P2Y4 receptors are expressed in pancreatic duct cells [16]. Because P2Y2 receptor mRNA was detected by RT-PCR in parotid duct cells (data not shown), the distribution of P2Y2 receptors was examined by immunohistochemistry. P2Y2 receptors were found in the apical region of the duct cells (Fig. 6C). These data suggest that P2Y2 receptors colocalize with IP_3R2 in the apical area of duct cells. Acinar cells expressed the P2Y2 receptors in the apicolateral area (Fig. 6C).

Discussion

Our results showed that acinar and duct cells expressed both SOC and non-SOC channels. M3 receptor stimulation of acinar cells activated SOC channels, given that a low concentration of Gd^{3+} partially inhibited the Ca^{2+} entry

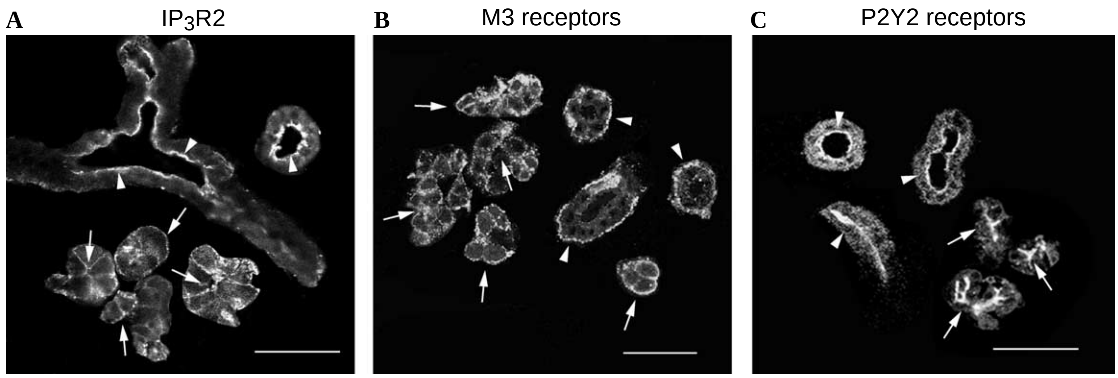

Fig. 6. (A) IP_3R2 in acini (arrows) and ducts (arrowheads). IP_3R2 is expressed in the basal and apicolateral areas of acini (arrows), but only in the apical region of ducts (arrowheads). (B) M3 receptors in acini (arrows) and ducts (arrowheads). Acinar cells express M3 receptors at the basal as well as apicolateral areas of acini (arrows). In duct cells, M3 is located only at the basal region (arrow heads). (C) P2Y2 receptors in acini (arrows) and ducts (arrowheads). P2Y2 receptors were located in the apicolateral region but not in the basal area of acini (arrows). On the other hand, P2Y2 receptors in ducts were observed only at the apical pole (arrowheads). Bars in A, B, and C indicate 50 μm.

(Fig. 4). In contrast, stimulation of the same receptor did not activate SOC channels in duct cells. However, this difference was not directly caused by the absence of SOC channels because store depletion by thapsigargin activated SOC channels in both cell types (Fig. 3). In addition, ATP could open Gd^{3+}-sensitive SOC channels in duct cells (Fig. 5). Thus, functional SOC channels were expressed in the duct cells, but were not sensitive to M3 receptor stimulation. ATP caused Ca^{2+} release from intracellular stores in duct cells (Fig. 5A). The present results showed that P2Y2 receptors were localized in the apical domain of duct cells (Fig. 6C). The distribution of P2Y2 receptors indicates that P2Y2 receptors colocalize with IP_3R2 near the luminal membrane of duct cells. Accordingly, ATP increased $[Ca^{2+}]_i$ in duct cells when it was applied to the apical side [17]. Thus, ATP released Ca^{2+} from intracellular stores and activated SOC and non-SOC channels in duct cells.

IP_3R2 was located in the apical area of duct cells (Fig. 6A). Consistent with our results, IP_3R2 of the duct cells in the parotid [7] and submandibular [15] gland is localized to the apical poles. In the present study, IP_3R2 was found beneath the basal and apicolateral membranes of the acinar cells. Previously, immunocytochemical experiments using tissue sections showed that parotid acinar cells express IP_3R2 in the apicolateral area [8,7] or in the apical pole [18]. We carefully re-examined the previous papers and found that the expression of IP_3Rs in the basal area was not very clear in these studies. Because the expression level of IP_3R2 in duct cells is rather high compared with acinar cells, as shown in Fig. 6A, the immunostaining of acinar cells in a tissue section may not have been fully analyzed in the previous experiments. Dissociating the acinar cells may be necessary to make a precise determination of the expression of IP_3R2. Re-examination of our previous data [8] also indicated that IP_3R2 was expressed in the basal region of acinar cells.

Our immunocytochemical experiments showed that M3 receptors had a restricted localization in the basal region, but were not in the apicolateral areas in duct cells (Fig. 6B). Xu et al. [17] have examined the localization of muscarinic receptors in duct cells of the submandibular salivary gland and showed that carbachol only increased the $[Ca^{2+}]_i$ of duct cells when it was applied to the basal side. Accordingly, the autonomic innervation of parotid ducts occurs at the basal side. Thus, M3 receptors are localized in the region of the basal membranes of duct cells. On the other hand, expression of the receptor was found in the apicolateral as well as the basal areas in acinar cells (Fig. 6B). The distribution of the M3 receptors in parotid acinar cells is quite similar to that of IP_3R2.

The microenvironment of intracellular signal cascades is important for intracellular signal transduction. On the apical membrane of the muscle sarcoplasmic reticulum, voltage-dependent Ca^{2+} channels contact ryanodine receptors. The opening of the voltage-dependent Ca^{2+} channel activates ryanodine receptors directly and induces intracellular Ca^{2+} release, which is necessary for excitation-contraction coupling [19–21]. In pancreatic acinar cells, a Ca^{2+} signaling complex composed of the M3 receptor and IP_3Rs exists in membrane microdomains [22]. Delmas et al. [23,24] have demonstrated that signaling microdomains define the specificity of the receptor-mediated IP_3 pathway in neurons. In their model, the bradykinin receptor and PLCβ cluster with the IP_3Rs, which activates TRPC1 (a SOC channel); in contrast, the M1 receptor and PLCβ build up in discrete domains where liberated IP_3 cannot activate the receptor; M1 receptor stimulation causes Ca^{2+} entry through TRPC6 (a non-SOC channel), which is activated by DAG. The present results indicate that IP_3R2 and M3 receptors colocalize in acinar cells, but not in duct cells (Fig. 7). When an M3 receptor binds ACh in the basal membrane of an acinar cell, PLCβ produces IP_3, which can promptly bind IP_3R2 on Ca^{2+} stores near the M3 receptor. Intracellular Ca^{2+} is released and extracellular Ca^{2+} enters the cell through SOC channels which may exist in the basal as well as apicolateral

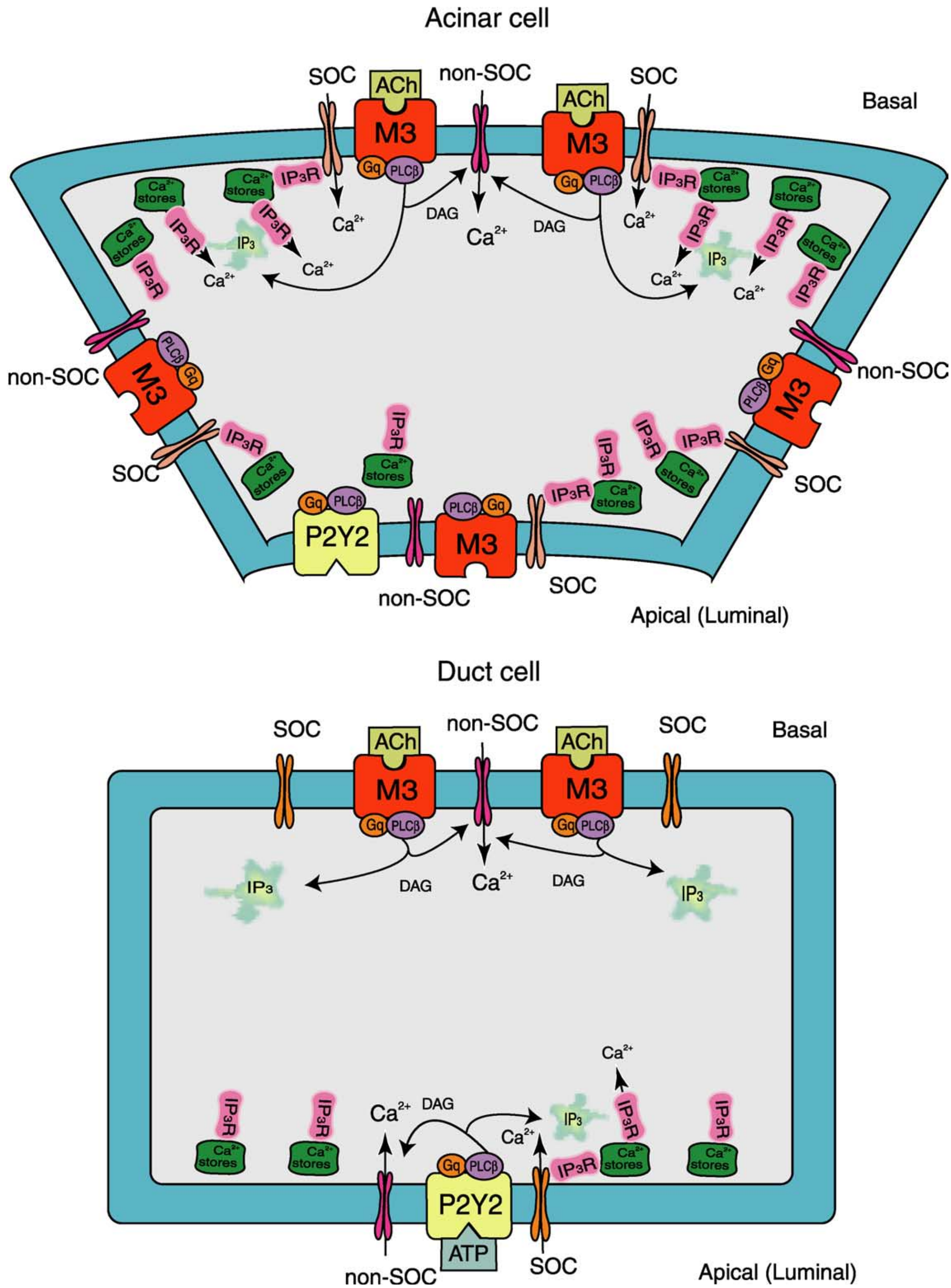

Fig. 7. In acinar cells, agonist stimulation of M3 receptors activates PLCβ via Gq proteins, resulting in the production of DAG and IP_3. DAG activates non-SOC channels and induces extracellular Ca^{2+} entry. IP_3 binds IP_3R2 and induces Ca^{2+} release from the intracellular stores, after which the store depletion activates SOC channels. In duct cells, stimulation of basal M3 receptors activates PLCβ and consequently opens non-SOC channels via DAG, but cannot release intracellular Ca^{2+} because IP_3R2 is located apically. On the other hand, ATP stimulates P2Y2 receptors, which results in the production of DAG and IP_3 at the apical membrane. DAG opens non-SOC channels and IP_3 releases Ca^{2+} from the IP_3-sensitive intracellular store. The store depletion of Ca^{2+} activates SOC channels.

membranes of acinar cells. PLCβ also produces DAG. DAG activates non-SOC channels, which may be located near M3 receptors. Because M3 receptor stimulation releases IP_3 near the basal membrane in duct cells, IP_3 may not reach the luminal IP_3R2. Thus, ACh fails to activate Ca^{2+} release from the intracellular stores. Because non-SOC channels were activated by M3 receptor stimulation, non-SOC channels may be located in the basal membrane of a duct cell. On the other hand, IP_3 released by apical P2Y2 receptor stimulation can reach the apical IP_3R2, which is followed by intracellular Ca^{2+} release and the activation of SOC channels. ATP induces DAG formation, which activates non-SOC channels. Thus, non-SOC channels may be located in the apical as well as basal membranes of duct cells. These signal transduction cascades in acinar and duct cells are given in Fig. 7.

Acknowledgment

We are grateful for the gift of the antibody against IP3 receptor type 2 from Dr. K. Mikoshiba (University of Tokyo, Tokyo, Japan).

Appendix A. Supplementary data

Supplementary data associated with this article can be found, in the online version, at doi:10.1016/j.bbrc.2005.07.200.

References

[1] M.J. Berridge, M.D. Bootman, H.L. Roderick, Calcium signalling: dynamics, homeostasis and remodelling, Nat. Rev. Mol. Cell Biol. (2003) 517–529.
[2] J.W. Putney Jr., R.R. McKay, Capacitative calcium entry channels, BioEssays (1999) 38–46.
[3] C. Montell, L. Birnbaumer, V. Flockerzi, The TRP channels, a remarkably functional family, Cell (2002) 595–598.
[4] D.E. Clapham, L.W. Runnels, C. Strübing, The trp ion channel family, Nat. Rev. Neurosci. (2001) 387–396.
[5] C. Hirono, T. Nakamoto, M. Sugita, Y. Iwasa, Y. Akagawa, Y. Shiba, Gramicidin-perforated patch analysis on HCO_3^- secretion through a forskolin-activated anion channel in rat parotid intralobular duct cells, J. Membr. Biol. (2001) 11–19.
[6] A. Dinudom, J.A. Young, D.I. Cook, Na^+ and Cl^- conductances are controlled by cytosolic Cl^- concentration in the intralobular duct cells of mouse mandibular glands, J. Membr. Biol. (1993) 289–295.
[7] A. Segawa, H. Takemura, S. Yamashina, Calcium signalling in tissue: diversity and domain-specific integration of individual cell response in salivary glands, J. Cell Sci. (2002) 1869–1876.
[8] H. Takemura, S. Yamashina, A. Segawa, Millisecond analyses of Ca^{2+} intiation sites evoked by muscarinic receptor stimulation in exocrine acinar cells, Biochem. Biophys. Res. Commun. (1999) 656–660.
[9] A. Segawa, S. Terakawa, S. Yamashina, C.R. Hopkins, Exocytosis in living salivary glands: direct visualization by video-enhanced microscopy and confocal laser microscopy, Eur. J. Cell Biol. (1991) 322–330.
[10] Y. Dai, I.S. Ambudkar, V.J. Horn, C.-K. Yeh, E.E. Kousvelari, S.J. Wall, M. Li, R.P. Yasuda, B.B. Wolfe, B.J. Baum, Evidence that M_3 muscarinic receptors in rat parotid gland couple to two second messenger systems, Am. J. Physiol. (1991) C1063–C1073.
[11] K. Sawaki, Y. Hiramatsu, B.J. Baum, I.S. Ambudkar, Involvement of Gaq/11 in m3-muscarinic receptor stimulation of phosphatidylinositol 4,5-bisphosphate-specific phospholipase C in rat parotid gland membranes, Arch. Biochem. Biophys. (1993) 546–550.
[12] L.M. Broad, T.R. Cannon, C.W. Taylor, A non-capacitative pathway activated by arachidonic acid is the major Ca^{2+} entry mechanism in rat A7r5 smooth muscle cells stimulated with low concentrations of vasopressin, J. Physiol. (1999) 121–134.
[13] Z. Moneer, C.W. Taylor, Reciprocal regulation of capacitative and non-capacitative Ca^{2+} entry in A7r5 vascular smooth muscle cells: only the latter operates during receptor activation, Biochem. J. (2002) 13–21.
[14] A.B. Parekh, J.W. Putney Jr., Store-operated calcium channels, Physiol. Rev. (2005) 757–810.
[15] M. Yamamoto-Hino, A. Miyawaki, A. Segawa, E. Adachi, S. Yamashina, T. Fujimoto, T. Sugiyama, T. Furuichi, M. Hasegawa, K. Mikoshiba, Apical vesicles bearing inositol 1,4,5-trisphosphate receptors in the Ca^{2+} initiation site of ductal epithelium of submandibular gland, J. Cell Biol. (1998) 135–142.
[16] X. Luo, W.Z. Zheng, M. Yan, M.G. Lee, S. Muallem, Multiple functional P2X and P2Y receptors in the luminal and basolateral membranes of pancreatic duct cells, Am. J. Physiol. (1999) C205–C215.
[17] X. Xu, J. Diaz, H. Zhao, S. Muallem, Characterization, localization and axial distribution of Ca^{2+} signalling receptors in the rat submandibular salivary gland ducts, J. Physiol. (1996) 647–662.
[18] X.J. Zhang, J.Y. Wen, K.R. Bidasee, H.R. Besch Jr., R.J.H. Wojcikiewicz, B. Lee, R.P. Rubin, Ryanodine and inositol trisphosphate receptors are differentially distributed and expressed in rat parotid gland, Biochem. J. (1999) 519–527.
[19] M.J. Berridge, Elementary and global aspects of calcium signalling, J. Physiol. (1997) 291–306.
[20] E. Rios, M.D. Stern, Calcium in close quarters: Microdomain feedback in excitation-contraction coupling and other cell biological phenomena, Ann. Rev. Biophys. Biomol. Struct. (1997) 47–82.
[21] D.M. Bers, Cardiac excitation–contraction coupling, Nature (2002) 198–205.
[22] Q. Li, X. Luo, S. Muallem, Functional mapping of Ca^{2+} signaling complexes in plasma membrane microdomains of polarized cells, J. Biol. Chem. (2004) 27837–27840.
[23] P. Delmas, N. Wanaverbecq, F.C. Abogadie, M. Mistry, D.A. Brown, Signaling microdomains define the specificity of receptor-mediated $InsP_3$ pathways in neurons, Neuron (2002) 209–220.
[24] P. Delmas, D.A. Brown, Junctional signaling microdomains: bridging the gap between the neuronal cell surface and Ca^{2+} stores, Neuron (2002) 787–790.